Motion of a Micro/Nanomanipulator using a Laser Beam Tracking System

Nabil Amari, David Folio, Antoine Ferreira

Motion of a Micro/Nanomanipulator using a Laser Beam Tracking System *

Nabil Amari, David Folio, and Antoine Ferreira†

INSA Centre Val de Loire, Université d'Orléans, PRISME EA 4229, Bourges, France
†antoine.ferreira@ensi-bourges.fr

Abstract. This paper presents a study of the control problem of a laser beam illuminating and focusing a microobject subjected to dynamic disturbances using light intensity for feedback only. The main idea is to guide and track the beam with a hybrid micro/nanomanipulator which is driven by a control signal generated by processing the beam intensity sensed by a four-quadrant photodiode sensitive detector (PSD). Since the pointing location of the beam depends on real-time control issues related to temperature variation, vibrations, output intensity control, and collimation of the light output, the 2-D beam location to the PSD measurement output must be estimated in real-time. To this aim a Kalman filter (KF) algorithm is designed to predict the beam location to perform efficient tracking and following control approach. Hence, a robust master/slave control strategy of the dual-stage micro and nanomanipulator system is presented based on sensitivity function decoupling design methodology. The decoupled feedback controller is synthesized and implemented in a 6-DoF micro/nanomanipulator allowing few centimeters displacement range with a nanometer resolution. A relevant case study, related to laser-beam tracking for imaging purposes, validates experimentally the proposed framework.

1 Introduction

High-precision position measurement systems based on laser beam reflection and/or transmission are commonly used in nanorobotics applications. In particular, laser beam nanomanipulation is useful tool to either characterize material properties of organic cells [1]; to study biological radiation effects on single cellular [1]; or interact with cells even in liquid environment [2]. Classically, a laser beam nanomanipulation platform is composed of the optical device, including the laser beam and sensor (eg. a camera or position sensitive detector (PSD)), and alignment mechanisms. The frame structure for maintaining the optical configuration allows precise controls positioning of the cells or micro robots. For instance, the Fig.1 illustrates the general microbeam system for radiation and transport tasks proposed in [1][2]. The main problem is then to focus the

* This work is carried out within the PIANHO project n°ANR-NANO-042 funded by the French National Agency (ANR) in the frame of its 2009 Programme in Nanosciences, Nanotechnologies and Nanosystems (P3N2009).

beam in a few micrometer size spots, and to control actively the beam direction to stabilize the beam at a desired location with a nanometer resolution. Such issues must be addressed when focusing a near-infrared laser beam at a nerve cell's leading edge [3],[4], when the laser beam perfectly tracks the moving atomic force microscope (AFM) probes [5] during manipulation tasks, or when the laser beam illuminates a microobject handled by a nanogripper for material characterization [6]. In the above mentioned cases, precise laser beam tracking of dynamic position with high-bandwidth rejection of disturbances produced by nanomanipulator platform vibration, piezoelectric actuator thermal drifts, photodetector noises, Brownian motion of laser beam and atmospheric turbulence are critical for the success of micro and nanomanipulation radiation tasks.

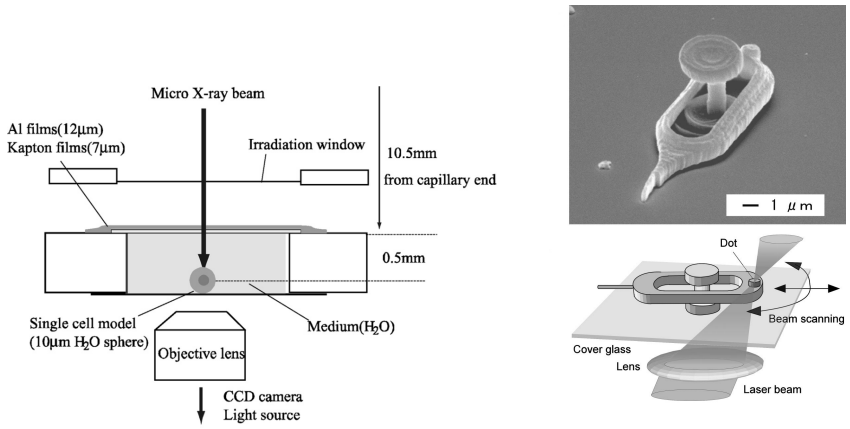

(a) (b)

Fig. 1. The microbeam system for radiation and transport: (a) model of single cell irradiation with micro X-ray beam[1]; and (b) optically driven micro tools in liquid for cellular manipulation[2](courtesy of[2]).

The single photodiode sensor (PSD) is currently being introduced in the nanomanipulation tasks, and used only for position measurement. Especially, the PSD is advantageous in terms of high speed response compared to the camera processing. In this paper we propose to use the PSD at the same time as indicator and feedback control in order to increase the overall performance and reliability of microbeam irradiation systems. The literature provides mainly two laser beam tracking configurations, that is steering i) the laser beam or ii) the photodetector. In the first case, some works propose to use fast tilt two-axis steering mirrors based on electrostatic MEMS actuators [7] or piezoelectric actuators with a fixed four-quadrant PSD. In the second case, the PSD is driven by a dual actuation system with robot micro/nano-manipulators [8], or x-y linear positioning stages

[9]. Whatever the technology involved, robust control of the laser beam tracking system is needed.

The purpose of this paper is to design a control system that rejects disturbances in the sense of minimizing the variance of the error in the position of the laser beam. The main idea is to track the emitting beam by processing the maximum beam intensity sensed by a four-quadrant PSD mounted on a 6 degree of freedom (DoF) dual-stage micro/nanomanipulator platform. Since the pointing location of the beam depends on real-time control issues related to disturbances, the laser beam position is estimated in real-time using the Kalman filter (KF) algorithm. To do so, a robust decoupled design controller is presented based on sensitivity function decoupling design methodology. The decoupled feedback controller is synthesized and implemented in a 6-DoF coupled magnetic and piezoelectric manipulation platform.
The paper is divided into five sections. Section 2 describes the experimental setup. Section 3 describes the dynamics modeling and system identification procedure and results. Section 4 describes the decoupled control design structure. Section 5 presents experimental results for the performance of the beam steering system.

2 Experimental Setup

The experimental setup of the beam pointing and tracking is shown in Fig.2. Two controllable micro/nano manipulators facing each other, composed of 3-DoF high-precision dual-stages, i.e., magnetic X-Y-Z closed-loop microstage (MCL Nano-Bio2M, from Physics Instruments) and piezoelectric x-y-z closed-loop nanostage (P-611.3S NanoCube, from Physics Instruments), respectively. Each pair micro/nano-manipulators constitute a compact computer-controllable system for X-Y-Z alignment (scanning) and positioning. In particular, the travel range of the microstage in the X-Y-Z directions is about few centimeters, while the fine motion of the nanostage is about 100μm. Thus, this dual-stage manipulator combines the advantages of ultra-high-resolution of the piezo-stage together with the long travel range of the micropositioning stages. The laser source is mounted on top of the nanostage (right manipulator) producing the laser beam. The main components of the beam steering experiment are a 635nm laser. A four-quadrant position sensing device (PSD) is mounted on top of the nanostage (left manipulator). The PSD measures the position of the image that the laser beam forms on a fixed plane.On the side view, a white light illuminates the workspace for top-view (optical microscope: Mituyo $\times$50) imaging for observing the laser beam when subjected to the micrometer variation and side-view (digital microscope: TIMM $\times$150) imaging used to observe the image of the laser beam in the operating region of the PSD. The sample platform is fixed on the system base.

Fig.3 shows the overall control scheme for power, laser beam tracking and micro/nano-manipulator control. The laser beam motion control (Brownian or stochastic trajectory) and measurement sequences are processed in real-time

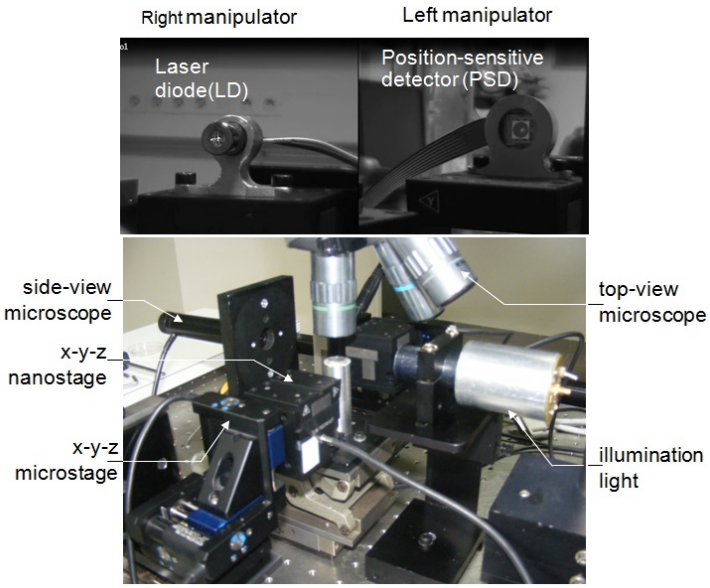

Fig. 2. Experimental setup.

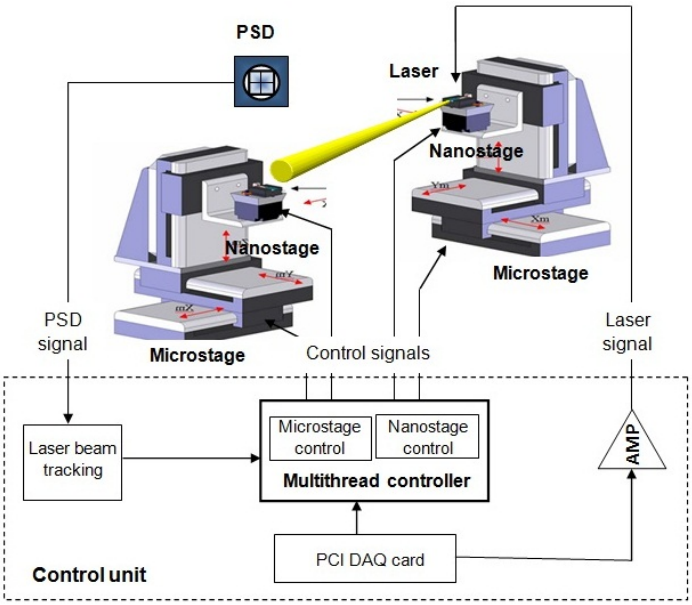

Fig. 3. Schematic diagram of the architecture of the laser beam tracking control system.

using MATLAB™ xPC software with a standalone target machine operating at a sample-and hold rate of 2kHz. A data acquisition (DAQ) (NI 6289) card is used for highspeed capturing of photodiode voltage output from a lock-in to detect maximum laser beam intensity and beam tracking. A multi-thread planning and control system is developed to independently manage the coordination during parallel laser beam motion and tracking, respectively.

3 Dynamics Modeling

This section reviews the different model dynamics of the different system components.

3.1 Dynamics of Piezoelectric and Magnetic Actuators

The first step for controller synthesis is to identify the model dynamics of the actuation platform. As no parametric information on drivers are available, an identification phase is needed to set up dynamic modeling of dual micro/nanostages. The piezoelectric 3-DoF nanostage and the magnetic 3-DoF microstage are deem as three-input and two-output (MIMO) system.

Thus, the modeling approach is based on system identification by experimental responses of micro/nano stages using a Pseudo Random Binary Sequence (PRBS) input signal. This input signal is implemented as a set of digital step signals with several operating points ranging from 0 to 100μm with an elementary step of about 10μm. The driving frequencies are lower than the first resonant mode of the nanostage system. The identification procedure is then realized using a closed loop response in order to protect the system submitted to large domain frequency, and subtract the model dynamic in open loop. To reduce the system order, the dynamic models of the micro (G_m) and nano (G_n) stages are chosen as a third-order approximation for each x-, y-, and z-axis, respectively,

$$G_{m(x,y,z)}(\mathsf{z}) = \frac{b_0 + b_1\mathsf{z}^{-1} + b_2\mathsf{z}^{-2} + b_3\mathsf{z}^{-3}}{1 + a_1\mathsf{z}^{-1} + a_2\mathsf{z}^{-2} + a_3\mathsf{z}^{-3}} \tag{1}$$

$$G_{n(x,y,z)}(\mathsf{z}) = \frac{b_1\mathsf{z}^{-1} + b_2\mathsf{z}^{-2} + b_3\mathsf{z}^{-3}}{1 + a_1\mathsf{z}^{-1} + a_2\mathsf{z}^{-2} + a_3\mathsf{z}^{-3}} \tag{2}$$

This choice was based on the correlation factor rate between the response of the model dynamics and the manipulators. The proposed optimized structure gives very high correlation factor values close to 99,5%. The obtained parameters values are listed in the Table 1.

The Fig.4 depicts the identification results of the dynamic responses and the identified model to the PRBS excitation signal along the x-axis of the microstage. Let us notice that a same behavior could be reported for the other axes. As one can see the identified model approximates suitably the system dynamics with an error close to 0.01 μm.

Table 1. Identified parameters of the dynamic models of the micro (G_m) and nano (G_n) stages for each x-, y-, and z-axis

Parameters	G_{mx}	G_{my}	G_{mz}	G_{nx}	G_{ny}	G_{nz}
a_1	0.4336	0.4363	0.4335	-0.00557	-0.00579	-0.000556
a_2	-0.36	-0.3599	-0.36	0.0196	0.025	0.0222
a_3	-0.162	-0.158	-0.171	-0.93	-0.997	-0.99999
b_0	0.9755	0.9755	0.9755	0	0	0
b_1	0.4769	0.48	0.46	0.00535	0.003	0.000556
b_2	-0.3779	-0.3559	-0.389	0.0271	0.00741	0.00535
b_3	- 0.168	- 0.201	- 0.156	0.0507	0.0117	0.00761

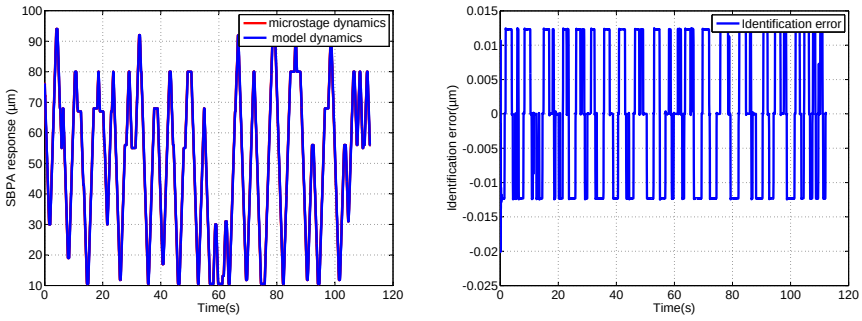

(a) (b)

Fig. 4. Identification results along the x-axis (a) micro stage dynamics when excited by a PRBS signal, and (b) the identification error.

3.2 Dynamics of Four Quadrant Detector

A four quadrant photo sensitive detector (PSD) has four photosensing parts arranged in four quadrants, respectively. When the elements are lighted by a beam of laser, they will generate currents according to the light intensity and then amplified into voltage signals. The combinations of voltages V_1 to V_4 can be used to indicate the offsets of the spot in relation to the center of the PSD as follows:

$$\begin{aligned} V_x &= (V_1 + V_4) - (V_2 + V_3) \\ V_y &= (V_1 + V_2) - (V_3 + V_4) \\ V_s &= V_1 + V_2 + V_3 + V_4. \end{aligned} \tag{3}$$

The V_x and V_y channel outputs are directly related to the energy of the laser beam that falls in each quadrant while V_s is the sum voltage. It is assumed that the light intensity on the laser's beam cross section obeys Gaussian distribution. The current generated by each sensing element can be described as given in:

$$I = k_1 \iint \frac{2E_l}{\pi^2 r} \cdot \mathrm{e}^{\frac{2(x_1^2+y_1^2)}{r^2}} \cdot dx_1 dy_1 \tag{4}$$

where I is the current, r the radius of the laser light spot, E_t is the energy of the laser beam, (x_1, y_1) is the coordinate of a point on the light spot in a coordinates system located at the center of the light spot, and k_1 is a coefficient. The calibration of the PSD is performed by moving the laser beam in the operating region of the fixed PSD. The Fig.5 presents an output voltage V_x measured by the PSD when the laser beam moves in the x-axis direction, wrt. the manipulator measured position. As one can see, in the operation region (small neighborhood of the aligned location), the photodiode voltage output V_x is approximately linearly related to light intensity units, with a negative slope. As the curve V_y is similar to that, it is omitted here. Obviously, when the spot is located in the sensing surface $V_x \neq 0$, $V_y \neq 0$ while if the spot is located in the center $V_x = 0$, $V_y = 0$. Moreover, we notice that there is a non-zero output at $x = 0$ due to the amplification of the noisy signals provided by the PSD sensor, which will be processed by the Kalman Filter (KF).

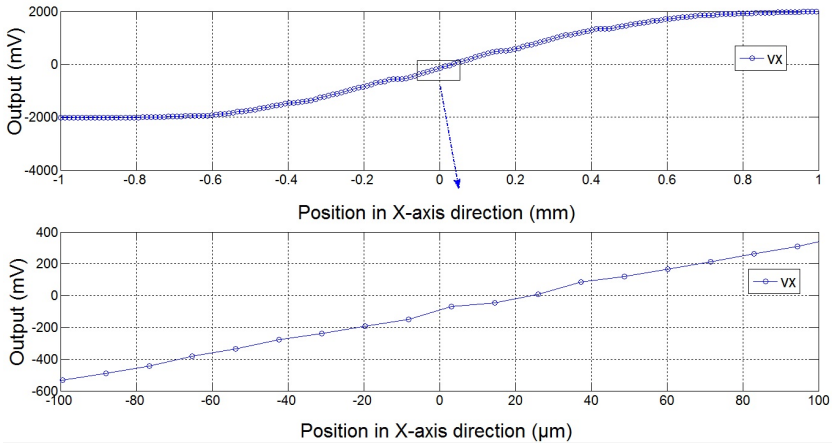

Fig. 5. Output voltage curve V_x with a zoom in the block area near zero on an four-quadrant PSD.

Furthermore, as one can see in Fig.6, the experimental intensity sensed by the PSD can be fitted with a Gaussian distribution as calculated by the theoretical equation (4).

3.3 Dynamics of Laser Beam Position

In this study, a dynamic disturbance is considered where the laser beam motion variation is assumed similar to the Brownian motion (represented in Fig. 7) of a particle subjected to excitation and frictional forces. The Brownian motion is applied as an input disturbance to the position of the laser beam carrier, and to

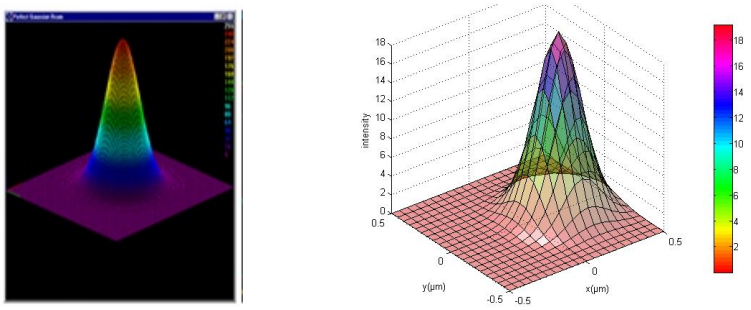

(a) (b)

Fig. 6. Light intensity on the laser's beam cross section: (a) theoretical and (b) experimental intensity obeying to Gaussian distribution.

the expected displacement measured by the PSD sensor. The Brownian motion is given by the following generalized differential equation:

$$\frac{d^2x(t)}{dt^2} + \beta_x \frac{dx(t)}{dt} = W_x \tag{5}$$

were β_x coefficient of friction and $W_x \sim N(0, \delta_x^2)$. To estimate with a discrete filter the laser beam positions at each sampling time t_k, a discrete model of the continuous dynamics (5) is necessary. In the x-axis the discretized equations of motion using a zero-order hold (zoh) are given by:

$$\dot{x}_k = \frac{x_k - x_{k-1}}{\Delta T}; \quad \ddot{x}_k = \frac{\dot{x}_k - \dot{x}_{k-1}}{\Delta T} \tag{6}$$

From (5) and (6), we obtain:

$$\dot{x}_k = \frac{\dot{x}_{k-1} + \Delta T W_{x_k}}{1 + \beta_x \Delta T} = a_x \dot{x}_{k-1} + b_x W_{x_k} \tag{7}$$

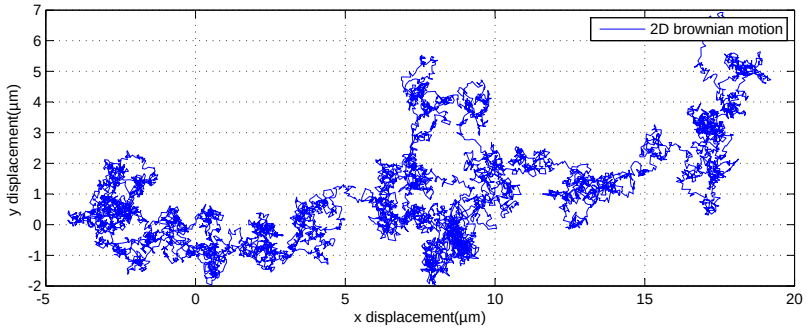

Fig. 7. Particle Brownian motion.

where ΔT is the discretization time step and the statistic properties of the excitation W_{x_k} force is assumed to be an zero-mean Gaussian random variable with variance δ_x^2. The y-axis can be modeled in the same manner as the x-axis, though with different dynamics. For 2D representation, the source state at discrete time k is defined as:

$$X_k = [x_k \ y_k \ \dot{x}_k \ \dot{y}_k]^T \tag{8}$$

(x_k, y_k) and $(\dot{x}_k, \dot{y}_k)$ are the source potion in the plane x-y and velocity respectively. The discrete state space of the Brownian laser beam is then represented by:

$$X_k = AX_{k-1} + BW_k \tag{9}$$

$$Y_k = CX_{k-1} \tag{10}$$

The state representation matrices $(A, \ B)$ are derived from the particle dynamics defined in (6)-(7) and $W_k \sim N(0, Q)$ is an zero-mean Gaussian random variable with matrix variance Q. It comes from (9) that:

$$X_k = \sum_{i=1}^{k} A^{k-i} B W_i + A^k X_0 \tag{11}$$

Because successive random variables W_i form *a priori* discrete zero mean white Gaussian process, X_k form(11) is Gaussian if the knowledge on X_0 is assumed Gaussian or equal to some fixed value. Its *a priori* variance at each step k can be calculated thanks to:

$$\sigma^2(X_k) = \sum_{i=1}^{k} A^{k-i} B \sigma^2(W_i) + A^k \sigma^2(X_0) \tag{12}$$

This equation (12) shows that bigger is the variance of W_k to set and bigger is the *a priori* uncertainty variance on the possible values of the modeled unknown position of the beam laser at t_k. Finally, the measurement Y_k of position takes into account the discrete-time white Gaussian noise V_k white zero mean and variance R added by the four quadrant photosensitive detector, that is:

$$Y_k = CX_{k-1} + V_k \tag{13}$$

4 Control Scheme of Beam Pointing and Tracking

4.1 Dual Micro/Nano-manipulator Controller

The problem considered here is to track the position variation of the laser beam into the x-y plane of the PSD by robust control commands sent to the dual micro/nano manipulators motions. The localization of the current laser beam position depends on the maximum beam intensity detection. Hence, a monitoring of the maximum intensity of the laser beam is needed[10]. It implies to

integrate a prediction model that anticipates the *a priori* laser beam motion, taking into account both dynamics, i.e, the laser beam and manipulators models. However, the different dynamics of the manipulators should be considered. The first actuator stage (microstage) has a large moving range but a low bandwidth while the second actuator stage (nanostage) has a high bandwidth but small moving range. The dual problem considered here is to know how to coordinate both micro and nanostages in order to track the laser beam motions using only signal position feedback delivered by the PSD. We adopted the master-slave control design to transform the dual-stage control design problem into decoupled or sequential multiple independent controller designed separately. The Fig.8 presents the master-slave control scheme to control two independent outputs of the micromanipulator G_m (1) and nanomanipulator G_n (2) systems by only one position feedback signal. This approach allows to combine the optical device with the micro-allignemnts mechanisms for an autonomous procedure especially when it comes to illuminates micro object under the focus of the laser beam for several minutes where the laser beam position is required or to limit the gripper deflexion in interaction with a microobject to not damage a flexible micro object and the gripper tool. Thanks to the master-slaver controller based to the mixed sensitivity, it is possible to fix the adapted dynamic performances of microstage using a simple proportional-derivative-integral (PID) controller in the C_m controller. To ensure robustness of the piezoelectric nanopositioning stages a H_∞ control scheme is implemented.

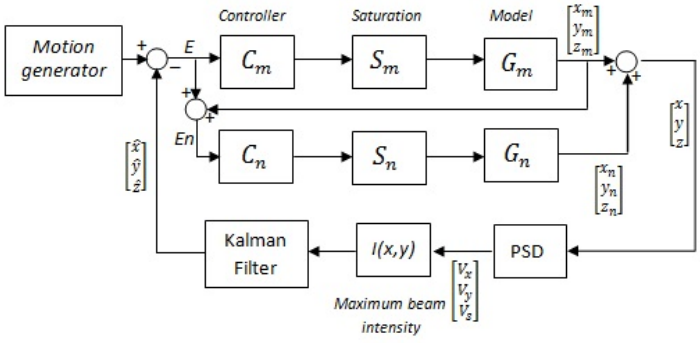

Fig. 8. Master-slave controller with decoupling structure for maximum light tracking.

4.2 Kalman Filter Estimator

In robotics, the Kalman filter (KF) is most suited to problems in tracking, localization, and navigation, and less so to problems in mapping[11][12]. This is

because the algorithm works best with well-defined state descriptions (positions, velocities, for example), and for states where observation and time-propagation models are also well understood. The prediction-estimation stages of the Kalman filter are derived from equations (9) and (13):
Prediction. A prediction $\hat{X}_{k|k-1}$ of the state at time k and its covariance $P_{k|k-1}$ is computed according to:

$$\hat{X}_{k|k-1} = A\hat{X}_{k-1|k-1} + BU_k \tag{14}$$

$$P_{k|k-1} = AP_{k-1|k-1}A^T + Q(k) \tag{15}$$

*Update.*At time k an observation $y(k)$ is made and the updated estimate $\hat{X}_{k|k}$ of the state X_k, together with the updated estimate covariance $P_{k|k}$, is computed from the state prediction and observation according to:

$$\hat{X}_{k|k} = \hat{X}_{k|k-1} + K_k(Y_k - C_k\hat{X}_{k|k-1}) \tag{16}$$

$$P_{k|k} = P_{k|k-1} - K_kS_kK_k^T \tag{17}$$

where the gain matrix K_k is given by:

$$K_k = P_{k|k-1}C_kS_k^{-1} \tag{18}$$

where

$$S_k = C_kP_{k|k-1}C_k + R_k \tag{19}$$

is the innovation covariance. The difference between the observation Y_k and the prediction observation $C_k\hat{X}_{k|k-1}$ is termed the innovation or residual $r(k)$. Thus, the input of the KF is the noisy measurement of the laser beam displacement in the x-y direction delivered by the photodiode detector and $\hat{X}_k$ is the output of the filter representing the estimation of the displacement at time t_k.

The Fig.9 illustrates a simulation result of the laser beam tracking using a Kalman filter. Here, the laser beam is animated with a synthetic Brownian motion. As one can see, the KF allows to estimate efficiently the laser beam motion.

5 Experiments

5.1 Dual Micro/Nano Manipulator Control Evaluation

First, the performance of the dual micro/nanomanipulator is evaluated using step response experiments with a reference set to 100 μm. Fig.10 illustrates the obtained step response of the x-axis of the : (a) nanostage with the H_∞ controller; (b) microstage with the Proportional-Derivative-Integral (PID) controller; and (c) master-salve controller where the decision of switching between microstage and nanostage, depends on the error resolution. At first glance, the dual micro/nano manipulator controller converges with no error to the reference,

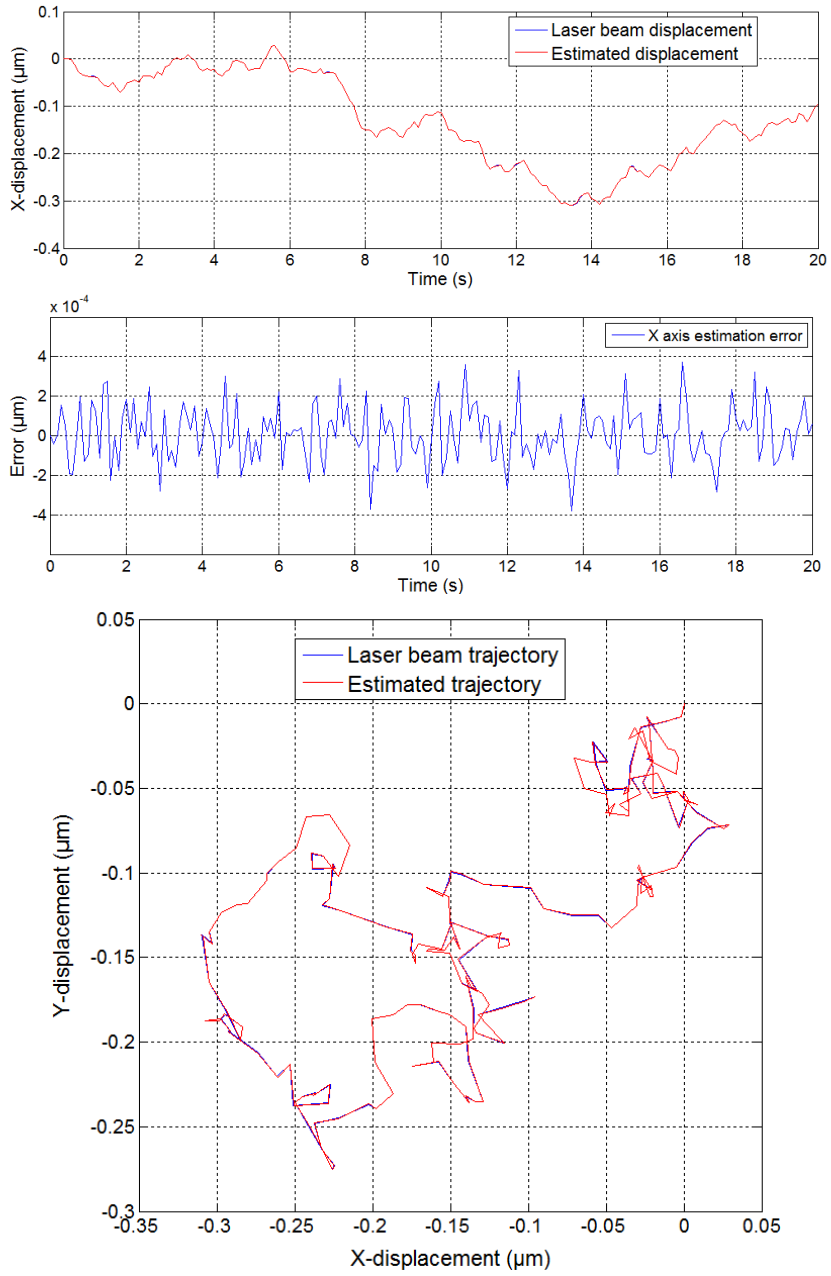

Fig. 9. Simulation of the laser beam tracking with the Kalman filter: motion estimation along the x-axis with its corresponding errors and the 2D displacement.

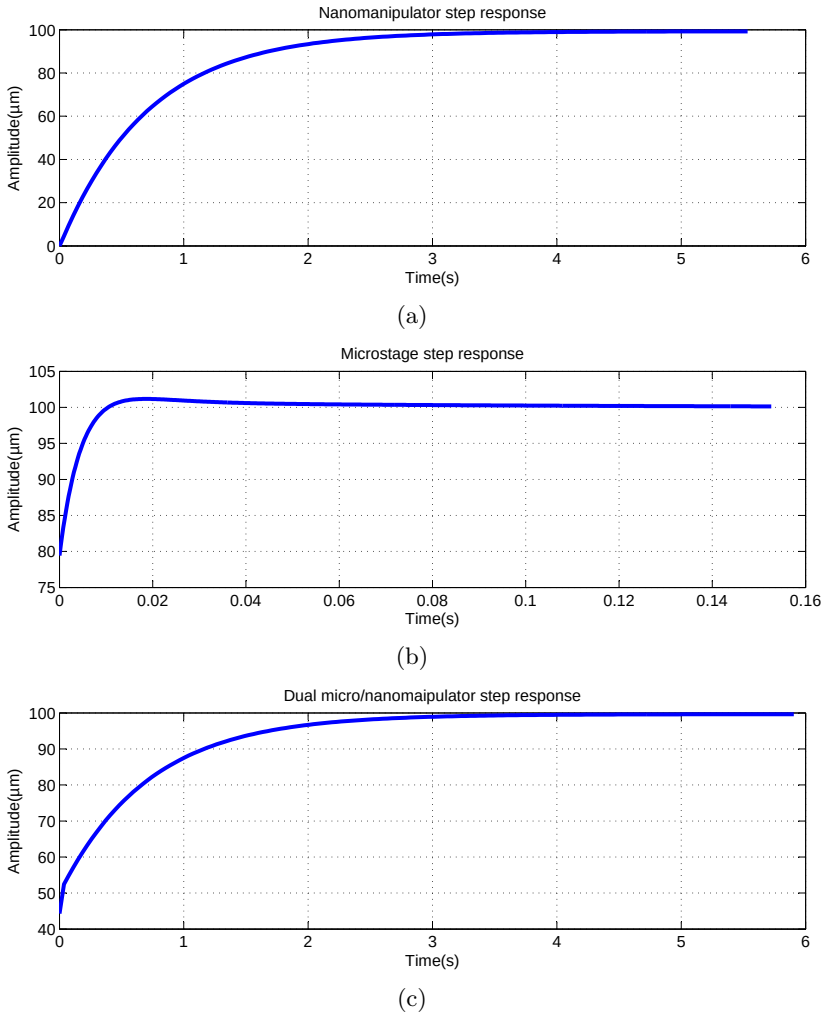

Fig. 10. Step responses of the (a) nanomanipulator, (b) nanomanipulator, micromanipulator and (c) dual controller.

with no overshoot, and with a settling time of about 4 s leading to a velocity of 25 μm/s.

The closed loop sensitivity function S_T defines the performance of the dual micro/nano-manipulator controller. Classically, in the frequency domain sensitivity S_T is equal to the sum of the closed loop sensitivity of the micromanipulator S_M and the nanomanipulator S_N (Fig.8), that is:

$$S_T = \frac{1}{1 + G_T} = S_N S_M \tag{20}$$

with

$$S_N = \frac{1}{1 + C_N G_N},\ S_M = \frac{1}{1 + C_M G_M} \tag{21}$$

The sensitivity of the dual micro/nano-manipulator demonstrates the possibility to design and combine the performances of each stage defined by their sensitivity function for control synthesis. First, the microstage is governed by a serial Proportional-Derivative-Integral (PID) controller formulated for each axis as:

$$C_M = K_p \frac{\tau_I s + 1}{\tau_I s}(\tau_D s + 1) \tag{22}$$

For the step response of the x-axis the PID parameters are set to: $K_{Px} = 140$, $\tau_{Ix} = 180$, $\tau_{Dx} = 120$. Secondly, the nanostage uses a H_∞ robust controller. Classically, the H_∞ synthesis problem is expressed as a matrix optimization problem, that is:

$$\min_k \|N(k)\|,\ N = [W_1 KS\ W_2 T\ W_3 S]^T \tag{23}$$

For a displacement in the x-direction of the nanomanipulator, the H_∞ synthesis allows to obtain a robust controller by using the following weighting functions:

$$\mathbf{W}_{1x} = \frac{s+1}{s+0.9258}, \qquad \mathbf{W}_{2x} = 0.7097, \qquad \mathbf{W}_{3x} = \frac{s+0.005935}{0.9613s+0.9032} \tag{24}$$

The optimized discrete transfer function of the x-axis nanomanipulator controller is then given by:

$$\mathbf{C}_{Nx}(z) = \frac{1.186z^4 - 4.01z^3 + 5.623z^2 - 3.953z + 1.154}{z^4 - 3.25z^3 + 4.405z^2 - 3.06z + 0.9044} \tag{25}$$

5.2 Laser Beam Motion Prediction

Secondly, the laser beam motion is estimated using the presented Kalman filter (KF) based on the identified Brownian model. To evaluate the performance of the KF, the laser beam is mounted on the right manipulator while the PSD sensor is mounted on the left manipulator, as depicted in Fig.2. Then, a random trajectory is generated to the laser beam before to initiate the laser beam tracking by the PSD sensor. The data rate of the sensor is $\Delta T = 2$. The KF parameters, i.e measurement noise matrix R, process noise matrix Q and initial state error matrix P_0, are defined as:

$$Q = 10^{-2}\mathbb{I}_{4\times4} + \begin{bmatrix} 0 & 2b_x^2 & b_x & b_x \\ 2b_x^2 & 0 & b_x^2 & b_x^2 \\ b_x & b_x & 0 & 2b^3 \\ b_x & b_x^2 & 2b_x^3 & 0 \end{bmatrix},\ \text{and}\ R = 10^{-4}\mathbb{I}_{2\times2}. \tag{26}$$

where $\mathbb{I}_{n\times n}$ is the $n \times n$ identity matrix. These noise matrices were chosen empirically in order to achieve the best performance of the filter.

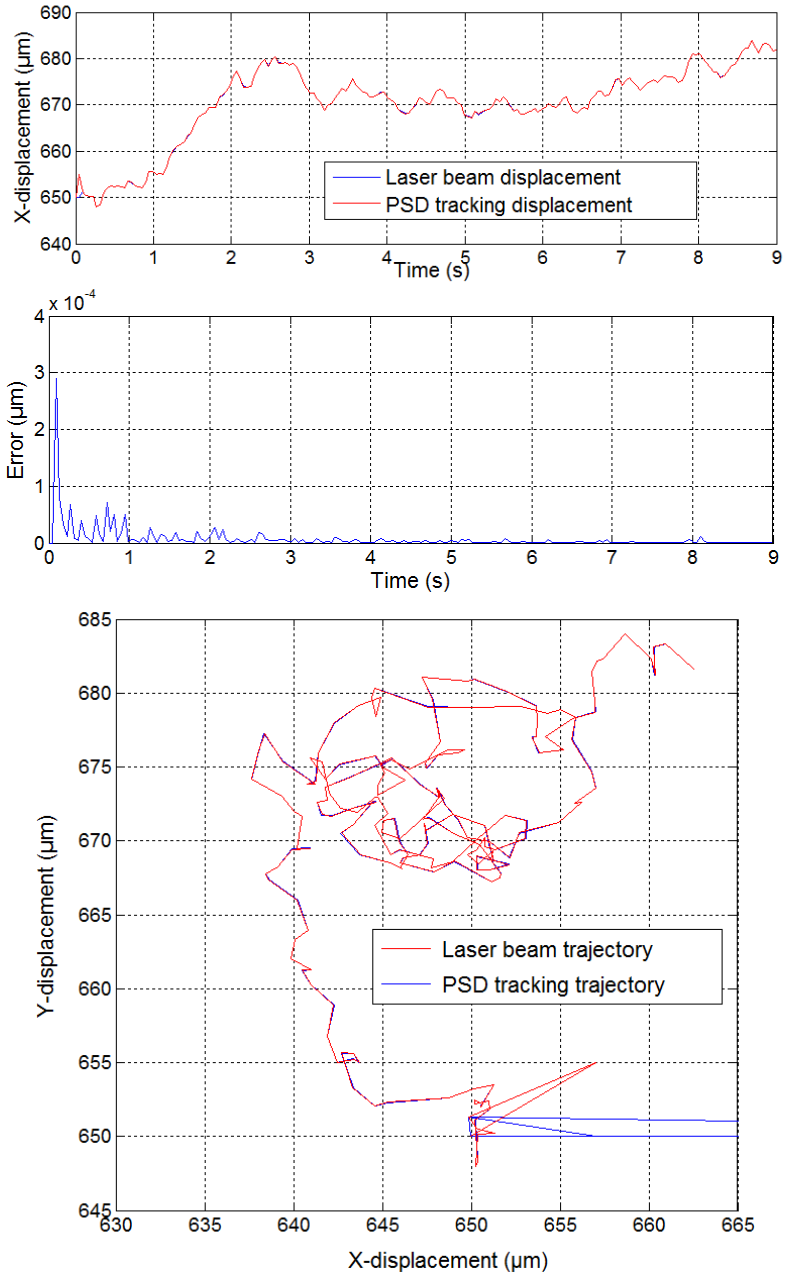

Fig. 11. Experimental tracking with Kalman filter: Motion estimation along x-y axis with corresponding errors and 2D displacement.

To evaluate the performance of Kalman filter, we settled the maximum intensity of the laser beam in the PSD center. The resulting estimation of laser beam motion prediction using KF is presented in Fig.11. The blue color represent the PSD trajectory resulting by the KF and red color the given variation in the position of the laser beam. At first glance, the KF succeed to reach quickly the real position, and to follow the laser beam motion variation very closely. As one can see in Fig.11(c), the PSD trajectory presents a convergence phase (bottom right part of the plot). This convergence step is due to the KF that has to reach its optimum prediction along with tracking the laser beam motions. As illustrated, the performances of the KF, in terms of precision, converge to the real position of the laser beam with a minimal estimation error around 0.01 nm. These results demonstrate clearly the sensitivity performances of the KF algorithm to detect and to estimate small variations of the laser beam motions.

5.3 Laser Beam Maximum Intensity Tracking

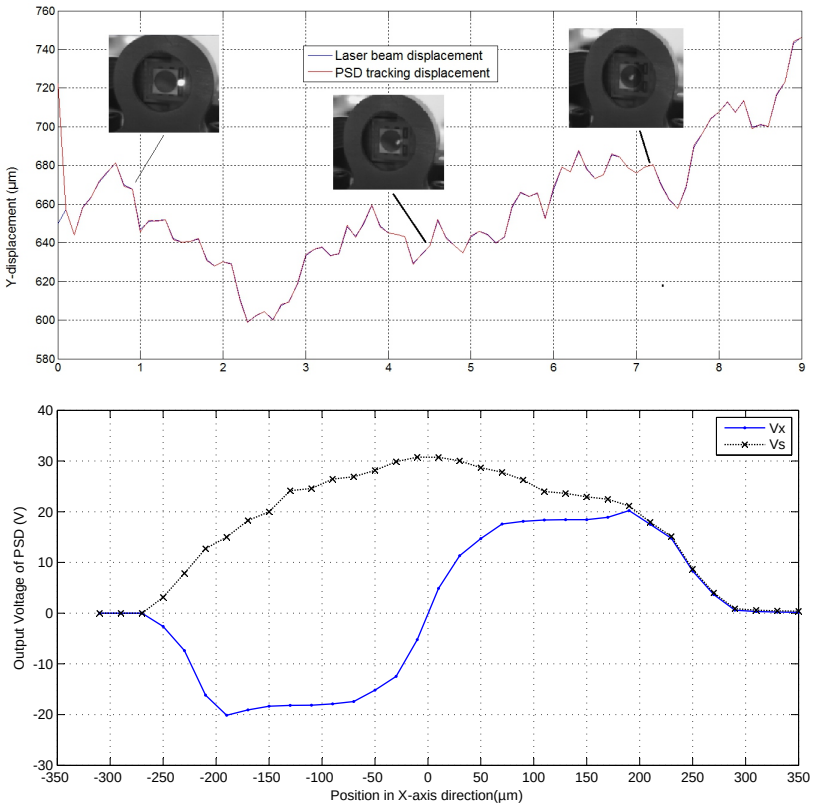

Fig. 12. Laser beam detection of maximum intensity.

In this scenario, the PSD has to track the laser beam motion, and find its maximum intensity. In addition here, the right manipulator move the laser beam with a composite motion defined by a constant displacement together with a Brownian motion. The resulting motion of the PSD along the y-axis is shown in Fig.12. These results illustrate a typical tracking task of a composite motion with a fast convergence time of the dual micro/nano-manipulator controller despite the constant bias displacement. Furthermore, the dual controller is able to find and to maintain the maximum beam light intensity in the center of the PSD against external perturbations. Let us also notice, that this approach assumes variations of laser light intensity during motion, measurement noise, and high motion dynamics. Moreover, these experiments demonstrate the robust estimation of the laser beam motion in real-time. As expected, the filtered estimate exhibits smaller variations. Finally, the master-slave controller with decoupled sensitivity is optimized in terms of tracking error.

6 CONCLUSION

This paper has presented a study on the control problem of a laser beam illuminating a target when subjected to dynamic disturbances using light intensity feedback. The main idea is to guide and track the beam with a hybrid micro/nanomanipulator which is driven by a control signal generated by processing the beam intensity sensed by a four-quadrant photodiode. The simulations and experiments demonstrated the efficiency of the approach when submitted to external disturbances, such as platform vibration, piezoelectric actuator thermal drifts, photodetector noises, brownian motion of laser beam and atmospheric turbulence. The use of a Kalman filter algorithm to estimate the laser beam motion has proven to be efficient despite the encountered high dynamics at such nanometer scale. Different experiments of single biological cell irradiation with a micro X-ray beam subjected to environmental perturbations are actually investigated with the proposed beam tracking system.

References

[1] S.Maruo, K.Ikuta,and H.Korogi,Submicron manipulation tools driven by light in a liquid, Applied Physics Letters 82,133(2003)

[2] T.Kuchimaru, F.Sato, Y.Higashino, K.Shimizu, Y.Kato, T.Iida, Microdosimetric Charecteristics of Micro X-ray Beam for Single Cell Irradiation.IEEE transaction on nuclear science vol53,no3,june2006.

[3] A. Ehrlicher, T. Betz, B. Stuhrmann, D. Koch, V. Milner, M. G. Raizen, and J. Kas, Proc. Natl. Acad. Sci. U.S.A. 99, 16024 (2002)

[4] B. Stuhrmann, M. Gogler, T. Betz, A. Ehrlicher, D. Koch, and J. Kas, Automated tracking and laser micromanipulation of motile cells, Rev. Sci. Instrum. 76, 035105 (2005)

[5] H. Xie , S. Régnier, High-Efficiency Automated Nanomanipulation with Parallel Imaging/Manipulation Force Microscopy, IEEE Transactions on Nanotechnology, Vol.11, Iss.1, pp:21-33, 2012.

[6] Pawel K. Orzechowski, James S. Gibson, Tsu-Chin Tsao, Optimal Disturbance Rejection by LTI Feedback Control in a Laser Beam Steering System, 43rd IEEE Conference on Decision and Control, December 14-17, 2004, Atlantis, Paradise Island, Bahamas, pp. 2143-2148.

[7] C.C. Lee, J. Park, Temperature Measurement of Visible Light-Emitting Diodes Using Nematic Liquid Crystal Thermography With Laser Illumination, IEEE Photonics Technology Letters, Vol. 16, NO. 7, July 2004.

[8] R. B. Evans, J.S. Griesbach, W.C. Messner, Piezoelectric microactuator for dual-stage control, IEEE Transactions on Magnetics, Vol.35, pp.977-981,1999.

[9] Nestor O. Perez-Arancibia, James S. Gibson, and Tsu-Chin Tsao, Observer-Based Intensity-Feedback Control for Laser Beam Pointing and Tracking, IEEE Transactions on Control Systems Technology, Vol.20, No.1, 2012, pp.31-47.

[10] Tran Trung Nguyen, A. Amthor and C. Ament, High Precision Laser Tracker System for Contactless Position Measurement, 2011 IEEE International Conference on Control System.

[11] R.E.Kalman, "A new approach to linear filtering and prediction problems". J.of bas.Engr.,vol.82,pp.35-45,1960.

[12] H.Durrant-Whyte, T.C. Henderson"Multisensor Data Fusion" Springer Handbook of robotics, 2008, pp 585-610